Nonlinear Analysis of Ultimate Capacity of Unbonded PC Shell Bridge using LECM

○Nagoya University, Member of JPCEA, Graduate Student, BONGOCHGETSAKUL Nattakorn
Nagoya University, Member of JPCEA, Professor, TANABE Tada-aki

Introduction

Concrete bridges that were constructed recently become more complicated in architectural apparent, functionality and design. Its mechanical behavior is consequently more complex and hardly to be estimated by traditional structural mechanics formulations. Prestressing system is introduced in designing of the concrete bridge results a thinner, stronger, and lighter structure. Those terms define sufficiently the structural performance of the structure. But in term of "safety", how much can we conclude that when will the structure fails, how it fails, and is the design load safe enough compared to the structural ultimate load capacity. Designing of prestressed concrete structures in general is performed based on an elastic analysis. Some engineers applied the safety factor to compensate an uncertainty in designing method, construction workmanship as well as nonlinearity of material and geometrical properties. However, how can we ensure that those selected safety factor and designing methods were corrected. Moreover, the complicated concrete structure, for example the PC box-section shell bridge, behaves in a very complicated way and its failure mode cannot be concluded based on only design drawing. Once the ultimate capacity and failure pattern of the structure accompanied with the design load are known, safety of the structure can be logically concluded. Not only the safety of the structure subjected to service load, but its maintenance planning, repairing and rehabitation are also possible applications.

In this paper, systematic procedures to estimate or predict the ultimate behavior and failure mode of the general unbonded prestressed concrete shell structures are presented. The application of the proposed method is shown through the analysis of PC box-type shell bridge, namely Kujira Bridge, which is made by thin prestressed concrete shell having a span-length of 100 meters. By the aid of a robust concrete constitutive equation, the Lattice Equivalent Continuum Model or LECM, applied to the nonlinear FEM program with a treatment of incompatibility of the unbonded prestressing tendon, complicated analysis of unbonded PC shell structures becomes possible.

Concrete governing model

The Lattice Equivalent Continuum Model, briefly called LECM, is used as constitutive equations to govern behaviors of the cracked concrete element (reinforced concrete). Basic concept of this model is representing concrete and reinforcement of a reinforced concrete element by a system of lattices that possess uniaxial properties of the corresponding lattice. Stress components relation between global stress field and those of the lattice system is considered by using a concept of micro-plane model. Unlike conventional tensorial models that relate the components of the stress tensor directly to the components of the strain tensor, micro-plane model work with stress and strain vectors on a set of planes of various orientations (so called microplane). The basic constitutive laws are defined on the level of the micro-plane and must be transformed to the material point using a certain relations between tensorial and vertorial components. Based on the microplane that changes its direction according to the propagation direction of concrete crack, stress-strain relation of corresponding lattice component can be appropriately expressed. Consequently, the complicated characteristics of cracked reinforced concrete element can be avoided. Moreover, by applying uniaxial properties to each lattice component, nonlinear behavior material even the more complicated hysteretic rules (loading-unloading behavior) of concrete and reinforcement can be independently defined. In addition, not only concrete and reinforcements that were been replaced by system of lattices, extra lattice system is needed to represent the contribution from shear transfer, which is one more feature of this model. Detailed formulation for each lattices system and material properties can be referred from reference papers.

Prestressing tendon formulation

The geometry of the tendon course is formulated based on local curvilinear coordinate system, which is possible for fully curved prestressing tendon. An embedded type tendon course is assumed, in which the tendon course can be freely defined on both in-plane and out-of-plane of the respected parent shell element, using the cubic interpolation function. The force components contributed from each tendon section are in both tangential and normal to the tendon alignment, in which the intermediate coordinate system, the so-called moving trihedral, is required to be calculated at any point along the tendon course. These force components are then carefully added to the parent internal force terms to retain a balance of the internal forces system. The stiffness contributed from prestressing tendon can be calculated by rotating the tendon axial stiffness to the global frame, and then added to the parent stiffness.

A free body diagram of segment of prestressing tendon passing an element is shown in the **Fig.1**. Let the tendon cross-sectional area is A_p having a tangential Young's modulus of E_{pt}. Both ends crossing the boundary of the element is defined by point P and Q, possessing tangential vector of $\mathbf{t}_P$ and $\mathbf{t}_Q$, respectively. Two internal prestressing forces, namely P_P and P_Q, are acting at these two ends. Component of distributed force along tangential direction is p_t, normal component heading to the center of curvature is p_n. These two distributed components can be written in

vector form as a vector $\mathbf{p}$. By using the prestressing tendon axial strain-displacement matrix, $\varepsilon_p = \mathbf{B}_p\mathbf{a}$, a virtual work equation for prestressing tendon can be written as in eq.(1).

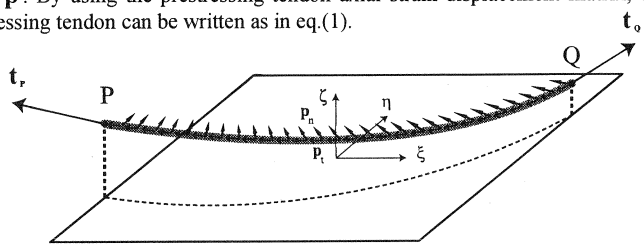

Fig. 1 Free body diagram of tendon segment

$$A_p\left[\int_\Gamma E_{pt}\mathbf{B}_p^T\otimes\mathbf{B}_p ds\right]\mathbf{a} + A_p\int_\Gamma \mathbf{B}_p^T\sigma_{p0}ds = \int_\Gamma \mathbf{N}^T\mathbf{p}dS + P_P\mathbf{N}_P^T\mathbf{t}_P - P_Q\mathbf{N}_Q^T\mathbf{t}_Q \tag{1}$$

Rewriting eq.(1) into more concise form, the equilibrium of prestressing tendon can be expressed as in the following equation.

$$\mathbf{K}_p\mathbf{a} + \mathbf{R}_p = \mathbf{P}_p \tag{2}$$

where

$$\mathbf{K}_p = A_p\int_\Gamma E_{pt}\mathbf{B}_p^T\otimes\mathbf{B}_p ds,\ \mathbf{P}_p = \int_\Gamma \mathbf{N}^T\mathbf{p}dS + P_P\mathbf{N}_P^T\mathbf{t}_P - P_Q\mathbf{N}_Q^T\mathbf{t}_Q,\ \mathbf{R}_p = A_p\int_\Gamma \mathbf{B}_p^T\sigma_{p0}ds \tag{3}$$

In bonded tendon prestressing system, the axial strain-displacement relation matrix $\mathbf{B}_p$ can be obtained by transform for parent strain field to the axial tendon strain respected to the moving trihedral. The parent strain field is defined in $\xi\eta\zeta$ coordinate system, which is equivalent to the strain field calculated from reinforced concrete element. The parent strain field is then transformed into moving trihedral system, **tnb** system, by using the transformation matrix, $\mathbf{T}$, as $\boldsymbol{\varepsilon}'_{tnb} = \mathbf{T}^T\boldsymbol{\varepsilon}_{\xi\eta\zeta}\mathbf{T}$.

Strain component that is considered in the tendon is only the axial component, ε'_x, which is corresponding to the tangential component, $\mathbf{t}$, of the moving trihedral. By removing the unwanted strain components, the tendon strain (axial strain) can be expressed as in the following equation.

$$\varepsilon_p = \mathbf{C}\left\{\varepsilon_\xi \quad \varepsilon_\eta \quad \varepsilon_\zeta \quad \gamma_{\xi\eta} \quad \gamma_{\xi\zeta} \quad \gamma_{\eta\zeta}\right\}^T = \mathbf{C}\boldsymbol{\varepsilon}_c = \mathbf{CB}\left[\mathbf{x}_p(t)\right]\mathbf{a} = \mathbf{B}_p(t)\mathbf{a} \tag{4}$$

where

$$\mathbf{B}_p(t) = \mathbf{CB}\left[\mathbf{x}_p(t)\right] \tag{5}$$

By a substitution of eq.(5) into eq.(3), stiffness matrix contributed by prestressing tendon for bonded problem can be obtained.

In the case of unbonded prestressing system, the $\mathbf{B}_p$ matrix is more complicated than as expressed by eq.(5). The total increment of concrete along the tendon length shall be equal to elongation of prestressing tendon, which can be mathematically expressed as

$$\int_0^l \varepsilon_c ds = \sum_{i=1}^n\left[\int_0^{l_i}\mathbf{CB}_i\left(\mathbf{x}_p(t)\right)ds\right]\mathbf{a}_i = \Delta u_p \tag{6}$$

where ε_c is concrete strain along the tendon length, l is a total length of prestressing tendon, n is a total number of element that prestressing tendon passing through, $\mathbf{B}_i$ is a strain-displacement matrix of parent element, and Δu_p is a total elongation of the prestressing tendon.

In the case of no friction if considered, tendon strain shall be the same through the length of tendon, that is

$$\varepsilon_p = \frac{\Delta u_p}{l} = \frac{\sum_{i=1}^n\left[\int_0^{l_i}\mathbf{CB}_i\left(\mathbf{x}_p(t)\right)ds\right]}{\sum_{i=1}^n\int_{-1}^{1}J_p dt}\mathbf{a} \tag{7}$$

Stiffness matrix for unbonded system, can also be calculated by using the eq.(7). Nevertheless, unlike the bonded case, integration range shall be done upon a total prestressing tendon length, in which the dimension of stiffness will be depending on the number of element that prestressing tendon passing through. Assembling of the stiffness matrix is performed component by component to the corresponding degree of freedom.

Analysis of the Kujira Bridge

A semi-arch type box-section prestressed concrete bridge located in Inagi district, Tokyo, is selected for a study of its ultimate behavior. The bridge, namely "Kujira Bridge", was a pedestrian prestressed concrete bridge that connects the Inagi main park to the Secondary Park located about 100 meters away. Cross-section of the bridge is a portal shape, as shown in **Fig. 2**. Its height and width vary from 5.960 *m*, 24.386 *m* at the support to 2.000 *m*, 16.800 *m* at the center, respectively. The bridge has a span length of 100.5 meters, supported by both fixed-end supports. Because of the completely fixed-ends, the bridge has a very high degree of statically indeterminate regarding prestressing in bridge axial direction.

Unbonded prestressing tendons (12T15.2) are located in five locations: top-slab at the support side, lower-slab at the bridge center, middle-wall inside the portal, sidewall inside the portal, vertical tendons at support, see **Fig. 3** for tendons alignment in the analysis model. The vertical tendons are used to fasten the bridge end to the support. However, instead of adopting the vertical tendons, end boundary conditions in the analytical model are fixed as a substitute. Thickness of the middle-wall and sidewall is moderately large so that these walls are functioned as a shear-resisting member. Due to its geometrical complexity, the ultimate behavior including failure mode cannot be predicted by traditional procedures.

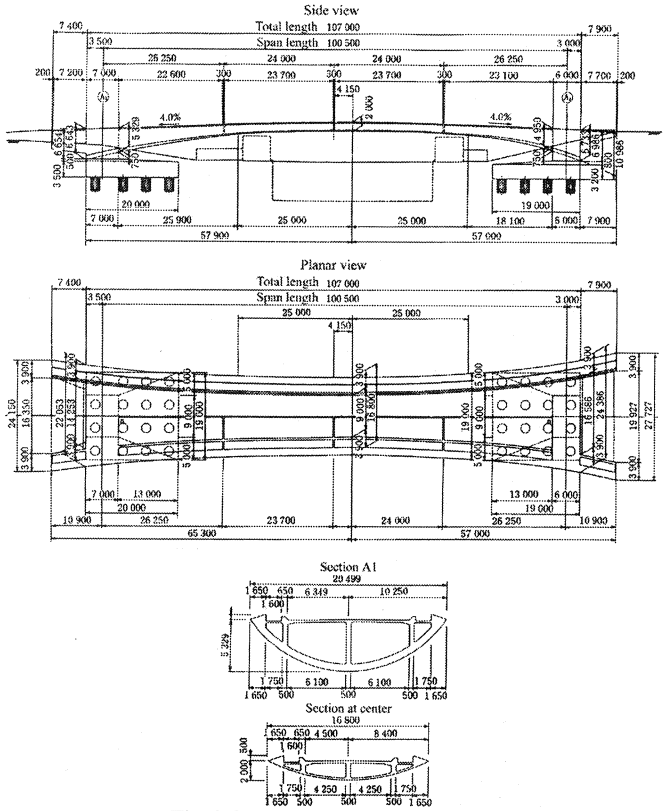

Fig. 2 Geometry of the Kujira Bridge

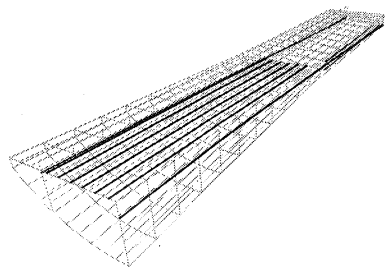

Fig. 3 FE mesh and tendons alignment

The bridge was analyzed by one-fourth model as shown in **Fig. 3** using 658 3D shell elements, in which ten independent unbonded tendons are introduced. Initial prestressing stress in each tendon is set to 900 N/mm^2. In the analysis, boundary conditions at the support are set to free prior to prestressing. The prestressing stress is gradually increased from zero to its proper limit (all the tendons at the same time). After the tendons have been prestressed, boundary conditions at the support are intermediately changed to a completely fixed type by keeping displacement at support constant. Boundary condition of the nodes elsewhere is set regarding the symmetry effect of the bridge. Distributed load is then applied on the edge of the middle-wall and sidewall. The total applied load and vertical displacement at the center of the bridge relation is shown in **Fig. 4**, including the analytical result when prestressing stress has been removed. At the stage just after tendons are fully prestressed, the mid-span is vertically deformed up about 74 *mm*. As mentioned previously, the support (the bigger cross-section) has not been fixed in the axis-direction at the prestressing phase. Thus, the bridge shrank a bit after prestressing is applied. Due to the application of vertical distributed load, the bridge bends back to it original stage when the load reached about 4788 kN. The structure continues to resist vertical load with stiffness close to its initial stiffness until the load reached about 11000 kN. With more application of the vertical load, stresses at the element near center of the bridge are changing from compression to tension state, stiffness of the bridge decreases gradually until the middle wall near the center failed. These concrete stress distribution conditions are shown in **Fig. 5**. The whiter color the more compression. Inversely, the darker color the more tension. The leftmost figure shows the state just after all tendons are prestressed. Middle figure show the stage when the bridge stiffness started to decrease. The rightmost show the ultimate state, with a failure of the middle wall near the bridge center. It can be seen from the stage just after prestressing (obviously in the top-slab at support side and in the lower-slab at the bridge center) that compressive stress concentrates at the element that the tendons passing through and gradually distributed to adjacent elements. Distribution

of tensile stresses can also be seen from the figure, but its scale does not cause any tensile crack. These compressive stresses change it stage gradually from minus to plus as the bridge is bending. At the stage just before failure, the stress distribution is very scatter due to partial stress concentration and difficulty to obtain the converged solution from the analysis. The bridge is finally failed by shear failure in the mid-wall near the center of the bridge, as shown in **Fig. 5**, with an ultimate load about 17000 kN. Comparing to the estimated design load, 10000 kN, the bridge is quite standing in the safe side. Regarding to the analytical result, ductility at ultimate is almost four times of that at design load level, strength at about 1.7 times. Sections of the bridge at the center and the support are deformed concavely as shown in the figure. In the analysis at ultimate stage, convergent of the solution was getting harder due to localized failure of the bridge. Convergent of the solution stop suddenly once the applied load reached about 17000 kN. This might caused by a very complicated deformation, for example, the snapback due to the complicated thin shell structure.

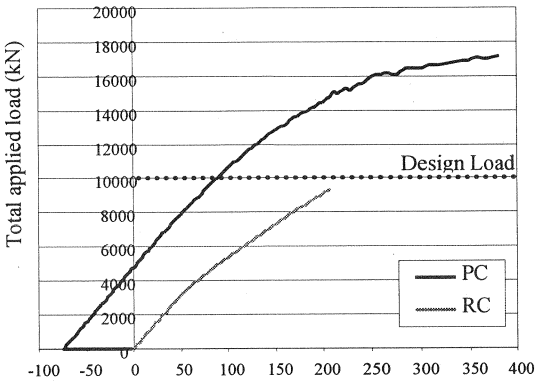

Fig. 4 Load-displacement relation

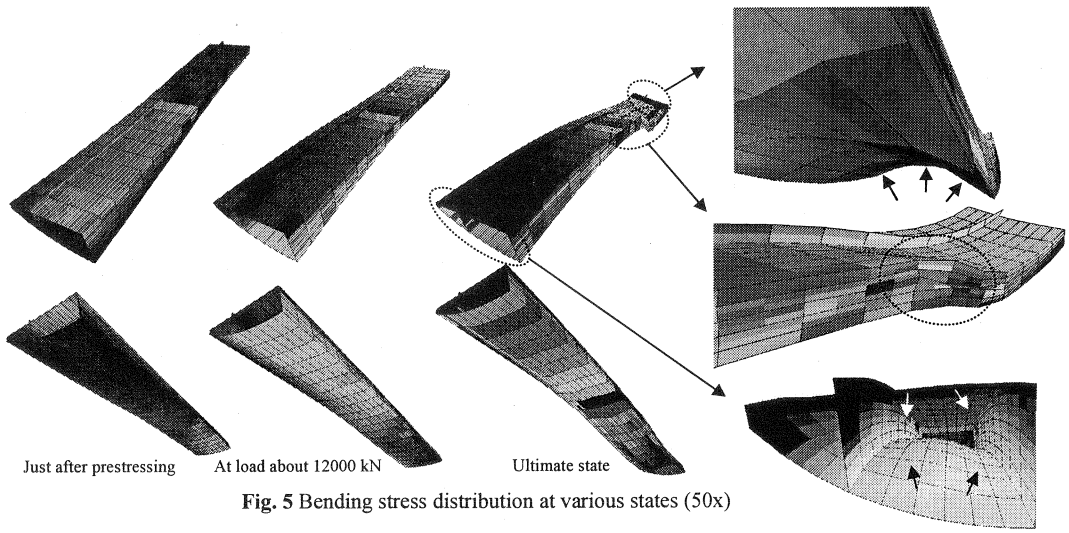

Fig. 5 Bending stress distribution at various states (50x)

Conclusion

Introducing of the prestressed concrete formulation accompanied with the reinforced concrete formulation (LECM) to the nonlinear FEM and shell formulation, the ultimate behavior of the unbonded prestressed concrete shell structure can be predicted which aids in safety judgment, maintenance and rehabitation planning of the concrete structure. Moreover, capability in predicting ultimate state of the structure is exceedingly needed in redesigning and finally yields safer and more reliable concrete structures.

References

1. Bongochgetsakul N. and Tanabe T., "Analysis of Box Type Shell Structures under Cyclic Loading by Lattice Equivalent Continuum Model", Transaction of JCI, Vol. 24, 2002, No. 2, pp. 949-954.
2. Bongochgetsakul N., Tanabe T., Itoh A., Phamavanh K., "Analysis of Unbonded Prestressed Concrete Structures by Lattice Equivalent Continuum Model", Transaction of JCI, Vol. 25, accepted 2003.